

# Summer warming during Heinrich Stadial 1 in Northeast China

Zeyang Zhu<sup>1,\*</sup>, Jing Wu<sup>1</sup>, Guoqiang Chu<sup>1,2</sup>, Patrick Rioual<sup>1,2</sup>, Jiaxin Lu<sup>3</sup>, Luo Wang<sup>1</sup>, and Jiaqi Liu<sup>1</sup><sup>1</sup>Key Laboratory of Cenozoic Geology Environment, Institute of Geology and Geophysics, Chinese Academy of Sciences (CAS), Beijing 100029, China<sup>2</sup>CAS Center for Excellence in Life and Paleoenvironment, Beijing 100044, China<sup>3</sup>School of Architecture and Geomatics Engineering, Shanxi Datong University, Datong 037000, China

## ABSTRACT

The last deglaciation is considered a key period for exploring the underlying dynamics of temperature changes because it was characterized by multiple millennial-scale abrupt climatic events. However, the limited number of quantitative temperature records in Northeast (NE) China covering the last deglaciation hampers a complete understanding of the mechanisms and processes behind the temperature changes that occurred in that region. Here, we present a quantitative reconstruction of summer temperature over the last deglaciation based on bacterial branched glycerol dialkyl glycerol tetraethers (brGDGTs) analyzed from the sediment sequence of Lake Kielguo, a small volcanic lake in NE China. The results show that summer temperature was lowest during the interval ca. 20–18.2 calibrated (cal.) k.y. B.P. with a value of  $\sim 11.1$  °C and increased by  $\sim 1.9$  °C during Heinrich Stadial 1 (HS1) and by  $\sim 2.7$  °C during the transition to the Bølling-Allerød (B-A). The summer temperatures during the B-A warm interval and Younger Dryas cold interval were  $\sim 14.1$  °C and  $\sim 12.0$  °C, respectively. The summer temperature record from the Lake Kielguo sediment sequence indicates that summer warming dominated the climate change state during HS1 in East Asia, which is different from the cooling pattern controlled by winter temperatures in the North Atlantic and Greenland realms. This distinction can be explained by weakened winter cooling signals triggered by the collapse of Atlantic Meridional Overturning Circulation when these signals propagated to East Asia, and increased summer temperature warming controlled by orbital and greenhouse gases during HS1 in East Asia.

## INTRODUCTION

The last deglaciation was characterized by abrupt millennial-scale climatic events such as Heinrich Stadial 1 (HS1) and the Younger Dryas (YD) superimposed on the gradual warming of global climate (Shakun and Carlson, 2010). HS1 (ca. 18–14.6 cal. k.y. B.P.), named for the cold interval containing Heinrich event 1, was known as the “Mystery Interval” because the temperature changes recorded during that period were decoupled from the trends in Northern Hemisphere summer insolation and CO<sub>2</sub> concentrations and from the Southern Hemisphere temperature changes (Denton, 2006). The cold conditions in the North Atlantic Ocean during HS1 were opposite to those recorded simultane-

ously in the Antarctic, as a consequence of the thermal bipolar seesaw (Stocker, 1998). Paleoclimatic records from Greenland (Buizert et al., 2014; Martin et al., 2023) and the North Atlantic Ocean (Darfeuille et al., 2016; Davtian and Bard, 2023) and climate simulations (He et al., 2021) all suggest cooling during HS1 triggered by the collapse of the Atlantic Meridional Overturning Circulation (AMOC). However, how the temperature changed in Northeast (NE) China and how the cooling signal was propagated to NE China during HS1 are still unclear due to the paucity of temperature records spanning that interval in that region. Increasing numbers of paleoclimatic records are being produced for NE China (Stebich et al., 2015; Zheng et al., 2017; Sun et al., 2018; Mingram et al., 2018; Zhu et al., 2021, 2023; Xu et al., 2023); however, most of these records only extend to the Bølling-Allerød (B-A) interval, and quantitative reconstructions


of temperature are scarce due to the limits of the proxy signals used in these studies.

Here, we present an independent temperature record spanning 20–10 calibrated (cal.) k.y. B.P. based on branched glycerol dialkyl glycerol tetraethers (brGDGTs; see Text S1 and Fig. S1 in the Supplemental Material<sup>1</sup>) from a small volcanic lake in NE China. This reconstruction provides an opportunity to better understand the temperature change history during the last deglaciation in NE China and the link between temperature changes in NE China and in the North Atlantic realm during the last deglaciation.

## MATERIAL AND METHODS

An 8.86 m sedimentary sequence, composed of two overlapping piston cores, was obtained using a piston corer from the center of Lake Kielguo (47°30.36'N, 120°51.99'E; Fig. 1; Text S3) in March 2007 (Wu et al., 2016). Twenty-one accelerator mass spectrometry (AMS) <sup>14</sup>C ages were obtained from the Poznan radiocarbon laboratory using terrestrial and aquatic plant macrofossils and bulk sediments (Table S1). The AMS <sup>14</sup>C ages were established using a Bayesian approach and the Bacon V2.2 software (Blaauw and Christen, 2011). More details about the chronology can be found in Zhu et al. (2023).

BrGDGTs were extracted from 0.5 to 1 g of freeze-dried sediment samples using an organic solvent composed of dichloromethane:methanol (9:1, v/v) mixture. The extracts were dried under N<sub>2</sub> and separated into polar and apolar fractions in a silica-gel chromatography column using methanol and *n*-hexane as the respective eluents. The polar fractions were dissolved in dichloromethane and passed through a 0.45 μm polytetrafluoroethylene filter. BrGDGT analyses were performed using high-performance liquid chromatography–atmospheric pressure chemical ionization–mass spectrometry (HPLC-APCI-MS),

Zeyang Zhu  <https://orcid.org/0000-0002-3933-5807>  
\*zhuzeyang@mail.iggcas.ac.cn

<sup>1</sup>Supplemental Material. The details about brGDGT-based proxy and Kielguo crater lake; chronological data; the comparison of different calibrations and different seasonal temperatures; and the comparison of TraCE-21ka results among different regions and different single-forcing. Texts S1–S3; Tables S1–S2; and Figures S1–S8. Please visit <https://doi.org/10.1130/G51881.1> to access the supplemental material; contact editing@geosociety.org with any questions.

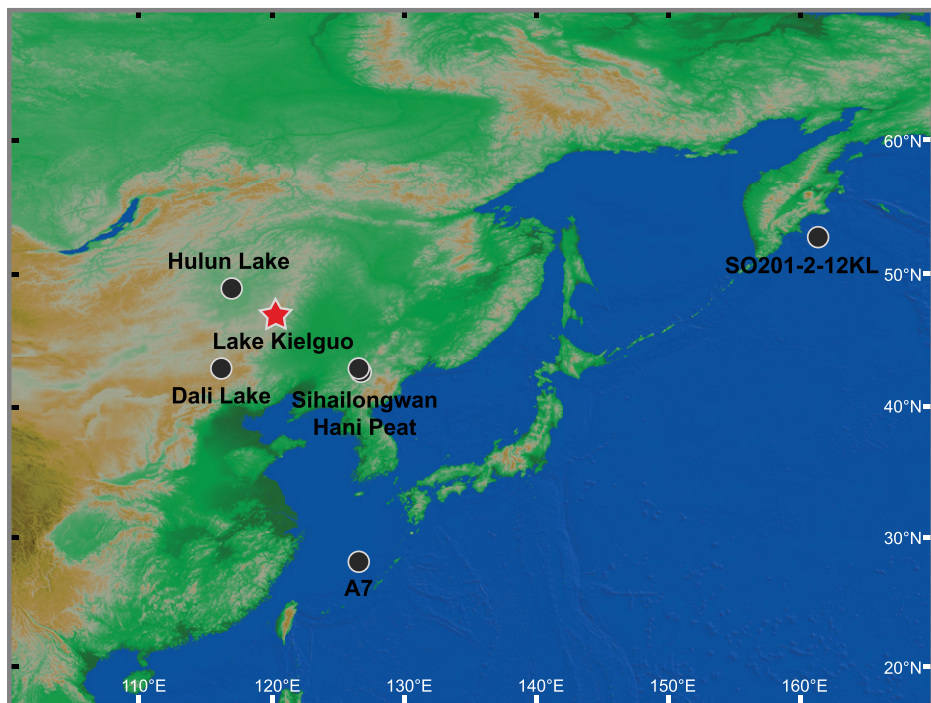


**Figure 1. Geographic locations of Lake Kielguo and other sites with paleoclimatic records mentioned in text.**

and the analysis followed the procedure of Zhu et al. (2023).

### RELIABILITY OF THE RECONSTRUCTED TEMPERATURE

It is necessary to validate the reliability of the analysis method and results because all the proxy data are indirect measurements of climate parameters. The calibration used in this study was a lacustrine brGDGT calibration to reconstruct the warm season temperature from Sun et al. (2011) (temperature =  $13.116 - 7.998 \times \text{CBT} + 27.752 \times \text{MBT}$ ; the CBT [Cyclization ratio of Branched Tetraethers] and MBT [Methylation index of Branched Tetraethers] are shown in Text S2), which was based on lake sediments from China and Nepal. The reasons for selecting this calibration have been discussed in detail elsewhere (Zhu et al., 2023), which can be summarized in three points. The first reason is that brGDGTs in Lake Kielguo sediments are produced mainly in situ (Fig. S2; Zhu et al., 2023), so the calibrations based on lake sediments are more suitable for Lake Kielguo. The calibration from Sun et al. (2011) was established based on samples from Lake Kielguo (which was named “Aershan Yuliang” in their lake list) and many other small, closed volcanic lakes in NE China similar to Lake Kielguo. The second reason is that the calculated results for the surface sediments from Lake Kielguo and two other lakes (Lake Luming and Lake Tuofengling), which are located in the same region, were more consistent with the meteorological data than those based on other calibra-

tions (Table S2). The last, but most important, reason is that the reconstructed temperatures obtained using this calibration for a short sediment core spanning the most recent past, from 1950 to 2020 CE, were remarkably consistent with the instrumental temperature record (Fig. S3; Zhu et al., 2023), giving a mean error between reconstructed and instrumental temperatures of  $\sim 0.4^\circ\text{C}$  (Fig. 2D).

BrGDGTs in Lake Kielguo record summer temperature rather than the mean annual temperature (MAT). This is supported by our investigation of the production of brGDGTs in Sihailongwan maar lake, another small, closed lake from NE China, which indicated that brGDGTs are produced mostly in summer and autumn rather than in winter, when the lake is covered by ice and snow (Zhu et al., 2021). Similar results showing that brGDGTs are produced during the warm season were obtained in other temperate lakes in China and elsewhere in the world, such as Donghu Lake (Qian et al., 2019) and Lower King Pond (Loomis et al., 2014). As such, the comparison among the meteorological MATs, different seasonal temperatures, and the brGDGT-based reconstructed temperatures also indicated that values were more consistent with the summer temperatures than with the mean annual and other seasonal temperatures (Fig. S4).

### TEMPERATURE CHANGES DURING THE LAST DEGLACIATION IN NE CHINA

During the interval between 20.0 and 10.0 cal. k.y. B.P., the summer temperatures based

on brGDGTs in Lake Kielguo varied between a low value of  $\sim 10.3^\circ\text{C}$ , which occurred ca. 18.0 cal. k.y. B.P., and a high value of  $\sim 16.4^\circ\text{C}$ , which occurred ca. 10.4 cal. k.y. B.P. (Fig. 2D). The coldest interval was ca. 20.0–18.0 cal. k.y. B.P., which corresponds to the late Last Glacial Maximum (LGM; Hughes, 2022), with a mean summer temperature of  $\sim 11.1^\circ\text{C}$ . After the first temperature shift ca. 18.0 cal. k.y. B.P., summer temperature increased gradually from  $\sim 11.1^\circ\text{C}$  to  $13.0^\circ\text{C}$  during the interval ca. 18.0–14.7 cal. k.y. B.P., which corresponds to HS1. This warming during HS1 was also suggested by the varve type record from Sihailongwan maar lake. More varves composed entirely of thick clastic laminae with pronounced winter clay layers (type 7) formed before ca. 18.0 cal. k.y. B.P., while varves with minerogenic clastic and rare occurrences of autochthonous organics (type 6) dominated during HS1 (Fig. 2E; Mingram et al., 2018). In addition, the pollen records from Xiaolongwan maar lake (Xu et al., 2023), Hulun Lake (Zhang et al., 2022), and Lake Kielguo (Wu et al., 2016) all suggested that the percentages of *Larix*, *Abies*, *Picea*, and *Pinus* species decreased slightly, while the percentages of *Betula* species increased, which indicates that the climate was more favorable during HS1 than during the LGM.

The second rapid temperature shift occurred ca. 14.7–14.4 cal. k.y. B.P., corresponding to the B-A transition, during which the summer temperature rose by  $\sim 2.7^\circ\text{C}$ . The summer temperature decreased slowly during the B-A from ca. 14.4 cal. k.y. B.P. to ca. 12.4 cal. k.y. B.P., when the mean value of  $\sim 14.1^\circ\text{C}$  was higher than that during HS1 and the LGM. Three short centennial-scale cool events occurred at ca. 14.1, ca. 13.5, and ca. 13.0 cal. k.y. B.P. (Fig. 2D). Other reconstructed temperatures in NE China also showed a warm B-A (Figs. 2A–2D).

The YD in NE China undoubtedly corresponded to a sharp cooling, as evidenced by all quantitative temperature records (Figs. 2A, 2B, and 2D) and pollen records (Wu et al., 2016; Zhang et al., 2022). At Lake Kielguo, the YD was also prominent with a mean summer temperature of  $\sim 11.7^\circ\text{C}$  during the interval ca. 12.4–11.5 cal. k.y. B.P., even though there was an abnormally high value at ca. 12.1 cal. k.y. B.P. (Fig. 2D). The summer temperature was cooler by  $\sim 1\text{--}3^\circ\text{C}$  during the YD than that during the B-A. The amplitude of the cooling recorded in the Kielguo record is therefore similar to the  $\sim 3^\circ\text{C}$  cooling recorded in the alkenone-based growing season temperature reconstruction from Sihailongwan (Fig. 2B) and to the  $\sim 2\text{--}3^\circ\text{C}$  drop recorded in the brGDGT-based MAT record from Hani peat (Fig. 2A). After the YD, the summer temperatures in Lake Kielguo increased rapidly and peaked ca. 10.5 cal. k.y. B.P. A similar warming trend was recorded in all the temperature archives

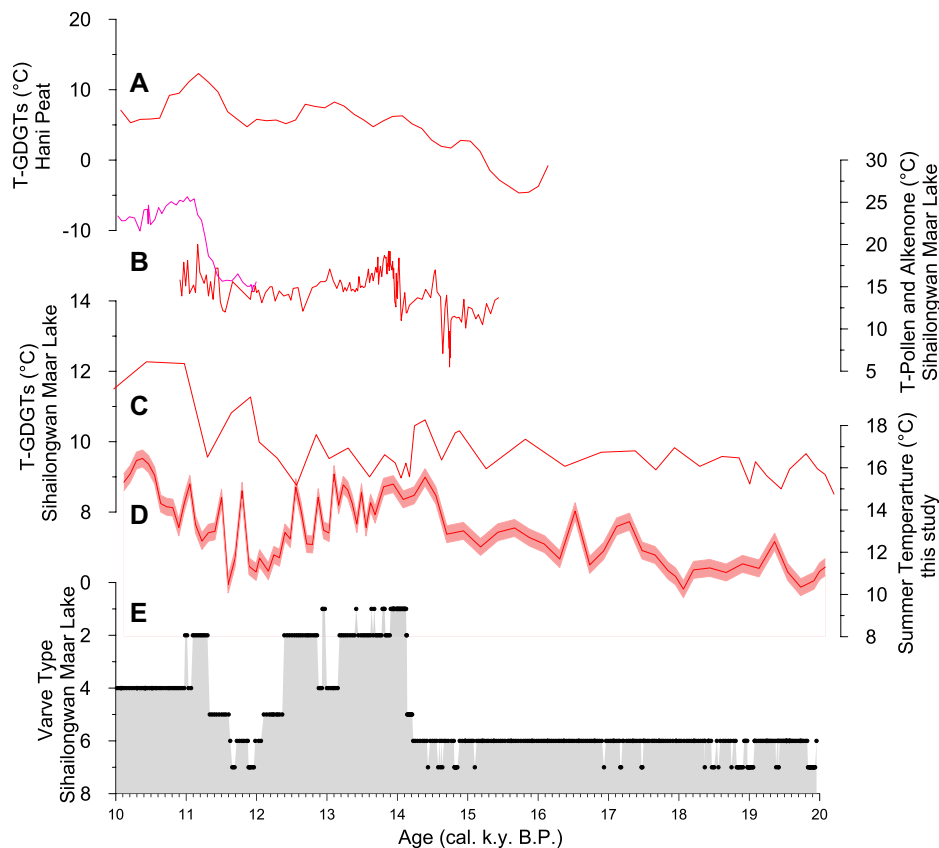


**Figure 2. Comparison of Kielguo record with other quantitative temperature (T) records from NE China and varve type record in Sihailongwan maar lake. (A) Glycerol dialkyl glycerol tetraethers (GDGT)–inferred mean annual temperature (MAT) from Hani peat (Zheng et al., 2017). (B) Alkenone-inferred growing season temperatures (red line; Sun et al., 2018), and pollen-inferred warmest month (July) temperatures (purple line; Stebich et al., 2015) from Sihailongwan maar lake. (C) The brGDGT-inferred mean summer and autumn temperatures from Sihailongwan maar lake (Zhu et al., 2021). (D) The brGDGT-inferred summer temperatures from Lake Kielguo (red shading is mean error). (E) Sihailongwan maar lake varve types (Mingram et al., 2018).**

from NE China, and the temperature peaked ca. 11.2–10.5 cal. k.y. B.P.

### COMPARISON OF TEMPERATURE CHANGES DURING THE LAST DEGLACIATION BETWEEN THE NORTH ATLANTIC AND NE CHINA

The summer temperature record from Lake Kielguo shows gradual summer warming during HS1, which is consistent with the gradual warming of MAT recorded by the brGDGT-based MAT records from Lake Tengchongqinghai, Southwest China (Tian et al., 2019) and Lantian loess profiles in North China (Gao et al., 2012; Lu et al., 2016) (Figs. 3E–3G). The summer warming during HS1 in NE China is also evidenced by changes in varve types from Sihailongwan and by pollen assemblages from Hulun Lake and Sihailongwan, which have been discussed previously herein. In addition, the summer warming during HS1 not only appeared in NE China, but the sea-surface temperature (SST) from the Northwest Pacific Ocean also increased during HS1 (Figs. 3H and 3I; Sun et al., 2005; Meyer et al., 2016). Furthermore, more ice-sheet meltwater flowed from Kamchatka into the North-

west Pacific Ocean and Okhotsk Sea during HS1, as indicated by the planktonic foraminifera  $\delta^{18}\text{O}$  record (Gorbarenko et al., 2019), which shows a temperature increase at that time. However, the winter temperature reconstruction from South China (Chu et al., 2017) presented a cooling pattern during HS1, different from the warming of MAT in East Asia. In summary, summer warming rather than winter cooling was the dominant climate state during HS1 in East Asia.

However, the temperature changed differently during HS1 in the North Atlantic realm. The reconstructed SST records based on alkenones and GDGTs (Darfeuil et al., 2016) showed prominent cooling in the North Atlantic during HS1 (Fig. 3B), and this cold interval was also archived in other paleorecords (Darfeuil et al., 2016) from the North Atlantic and Greenland. In addition, the Greenland temperature reconstruction based on the gas-phase  $\delta^{15}\text{N-N}_2$  values in ice cores (Buizert et al., 2014) also shows a slight cooling during the early HS1 compared to the LGM (Fig. 3C). Although the HS1 cold event is apparently absent in the Greenland ice-sheet  $\delta^{18}\text{O}$  record (Fig. 3D), it has been suggested that the HS1 cooling did indeed occur over the Arctic in winter (He et al.,

2021). It is accepted that winter temperature was a dominant control on the climate state during the last deglaciation in the North Atlantic (Buizert et al., 2018; He et al., 2021), different from the climate state dominated by summer warming in East Asia. The seasonality of the abrupt climate change has shown that the abrupt temperature changes were weighted toward the winter during Heinrich Stadials (Denton et al., 2022). The abrupt collapse of the AMOC recorded by sedimentary  $^{231}\text{Pa}/^{230}\text{Th}$  values in marine sediment core OCE326-GGC5 (Fig. 3A; McManus et al., 2004) was considered to be the trigger of this cold interval, in spite of some records that suggested different manifestations of the AMOC during HS1 (Repschläger et al., 2021). The response to the AMOC variations is weaker in summer than in winter due to the amplification by sea-ice extent (Flückiger et al., 2008). In addition, TraCE-21ka model simulations also show more dramatic temperature changes in winter than in summer during the last deglaciation in the North Atlantic (Fig. 4A), while slight winter temperature and dramatic summer temperature changes are found in NE China (Fig. 4B).

The reason for the different seasonal temperatures dominant in NE China and in North Atlantic and Greenland realms is that the dominant winter cooling signal triggered by the collapse of the AMOC from the North Atlantic weakened when it was propagated to East Asia, and it was suppressed by the increases in insolation and greenhouse gas concentrations. The TraCE-21ka model meltwater single forcing simulations show that the winter temperature changed by  $\sim 23^\circ\text{C}$  during the last deglaciation in Greenland and only by  $\sim 4^\circ\text{C}$  in NE China (Figs. 4C and 4D), which suggests that the winter cooling signal weakened when it was propagated to NE China. The summer temperature changes influenced by AMOC also decreased from Greenland to NE China (Figs. 4C and 4D). In contrast, the increase in summer temperatures controlled by orbital forcing in NE China was more than that in Greenland (Figs. 4E and 4F). The increases in greenhouse gases forced the summer and winter temperatures to increase during HS1 both in Greenland and NE China, but the winter temperature changes were more remarkable in Greenland (Fig. S7). The ice forcing weakly influenced the temperature changes during HS1 both in Greenland and NE China (Fig. S8).

In conclusion, we presented a quantitative summer temperature record based on brGDGTs over the last deglaciation from NE China, which indicated that the climate change state during HS1 was dominated by summer warming in East Asia, different from the cooling pattern controlled by winter temperatures in the North Atlantic and Greenland realms. This distinction is due to the fact that the winter cooling signal triggered by the collapse of the AMOC was attenuated as it propagated to East Asia, and



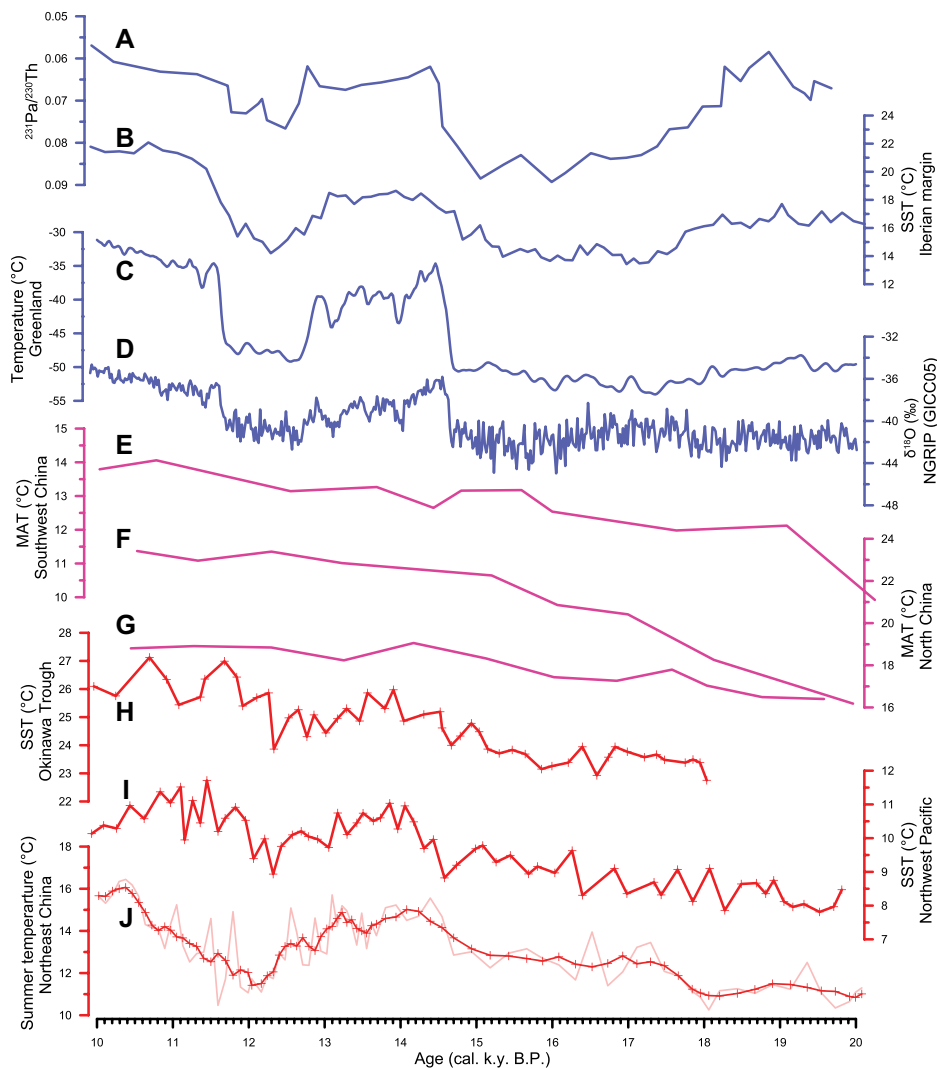


**Figure 3. Forcing factors and comparison among records from North Atlantic, Greenland, northeastern Pacific, and Northeast China. (A)** Sedimentary  $^{231}\text{Pa}/^{230}\text{Th}$  in marine sediment core OCE326-GGC5 as proxy for Atlantic Meridional Overturning Circulation (AMOC) intensity (McManus et al., 2004). **(B)** Alkenone unsaturation ratio ( $U^{k}_{37}$ ) sea-surface temperature (SST) record from marine core MD95-2042 from Iberian margin (Darfeuil et al., 2016). **(C)** Greenland temperature reconstruction based on gas-phase  $\delta^{15}\text{N}-\text{N}_2$  in ice cores (Buizert et al., 2014). **(D)** North Greenland Ice Core Project (NGRIP) ice-core  $\delta^{18}\text{O}$  record at GICC05 (Svensson et al., 2008). **(E)** Branched glycerol dialkyl glycerol tetraethers (brGDGT)-based mean annual temperature (MAT) record from Lake TengchongQinghai, Southwest China (Tian et al., 2019). **(F–G)** brGDGT-based MAT records from Lantian loess profiles in North China (Gao et al., 2012; Lu et al., 2016). **(H)** Mg/Ca SST record from core A7 from middle of Okinawa Trough (Sun et al., 2005). **(I)** Tetraether index of 86 carbon atoms ( $\text{TEX}^{\text{L}}_{86}$ ) SST record from core SO201-2-12KL, Northwest Pacific (Meyer et al., 2016). **(J)** The brGDGT-based summer temperature record from Lake Kielguo at NE China (this study).

the summer warming controlled by orbital and greenhouse gases dominated the temperature changes during HS1 in East Asia.

#### ACKNOWLEDGMENTS

This work was funded by the National Key Research and Development Program of China (grant no. 2023YFF0804702), the National Natural Science Foundation of China (41972190, 42030507), and the Strategic Priority Research Program of Chinese Academy of Sciences (XDB 26000000). We acknowledge the use of the refrigeration facility at the Beijing National Observatory of Space Environment, Institute of Geology and Geophysics, Chinese Academy of Sciences, Beijing, China.

#### REFERENCES CITED

- Blaauw, M., and Christen, J.A., 2011, Flexible paleoclimate age-depth models using an autoregressive gamma process: Bayesian Analysis, v. 6, p. 457–474, <https://doi.org/10.1214/ba/1339616472>.
- Buizert, C., et al., 2014, Greenland temperature response to climate forcing during the last deglaciation: Science, v. 345, p. 1177–1180, <https://doi.org/10.1126/science.1254961>.
- Buizert, C., Keisling, B.A., Box, J.E., He, F., Carlson, A.E., Sinclair, G., and DeConto, R.M., 2018, Greenland-wide seasonal temperatures during the last deglaciation: Geophysical Research Letters, v. 45, p. 1905–1914, <https://doi.org/10.1002/2017GL075601>.

- Chu, G., Sun, Q., Zhu, Q., Shan, Y., Shang, W., Ling, Y., Su, Y., Xie, M., Wang, X., and Liu, J., 2017, The role of the Asian winter monsoon in the rapid propagation of abrupt climate changes during the last deglaciation: Quaternary Science Reviews, v. 177, p. 120–129, <https://doi.org/10.1016/j.quascirev.2017.10.014>.
- Darfeuil, S., Ménot, G., Giraud, X., Rostek, F., Tachikawa, K., Garcia, M., and Bard, É., 2016, Sea surface temperature reconstructions over the last 70 kyr off Portugal: Biomarker data and regional modeling: Paleoceanography, v. 31, p. 40–65, <https://doi.org/10.1002/2015PA002831>.
- Davtian, N., and Bard, E., 2023, A new view on abrupt climate changes and the bipolar seesaw based on paleotemperatures from Iberian margin sediments: Proceedings of the National Academy of Sciences of the United States of America, v. 120, <https://doi.org/10.1073/pnas.2209558120>.
- Denton, G.H., 2006, The mystery interval 17.5 to 14.5 kys ago: PAGES News Letter, v. 14, p. 14–16, <http://ci.ni.ac.jp/naid/10025190455/en/>.
- Denton, G.H., Toucanne, S., Putnam, A.E., Barrell, D.J.A., and Russell, J.L., 2022, Heinrich summers: Quaternary Science Reviews, v. 295, <https://doi.org/10.1016/j.quascirev.2022.107750>.
- Flückiger, J., Knutti, R., White, J.W.C., and Renssen, H., 2008, Modeled seasonality of glacial abrupt climate events: Climate Dynamics, v. 31, p. 633–645, <https://doi.org/10.1007/s00382-008-0373-y>.
- Gao, L., Nie, J., Clemens, S., Liu, W., Sun, J., Zech, R., and Huang, Y., 2012, The importance of solar insolation on the temperature variations for the past 110kyr on the Chinese Loess Plateau: Palaeogeography, Palaeoclimatology, Palaeoecology, v. 317–318, p. 128–133, <https://doi.org/10.1016/j.palaeo.2011.12.021>.
- Gorbarenko, S., Shi, X., Zou, J., Velivetskaya, T., Artemova, A., Liu, Y., Yanchenko, E., and Vasilenko, Y., 2019, Evidence of meltwater pulses into the North Pacific over the last 20 ka due to the decay of Kamchatka glaciers and Cordilleran ice sheet: Global and Planetary Change, v. 172, p. 33–44, <https://doi.org/10.1016/j.gloplacha.2018.09.014>.
- He, C., Liu, Z., Otto-Bliessner, B.L., Brady, E.C., Zhu, C., Tomas, R., Buizert, C., and Severinghaus, J.P., 2021, Abrupt Heinrich Stadial 1 cooling missing in Greenland oxygen isotopes: Science Advances, v. 7, <https://doi.org/10.1126/sciadv.abh1007>.
- Hughes, P.D., 2022, Concept and global context of the glacial landforms from the Last Glacial Maximum, in Palacios, D., et al., eds., European Glacial Landscapes: Amsterdam, Netherlands, Elsevier, p. 355–358, <https://doi.org/10.1016/B978-0-12-823498-3.00039-X>.
- Loomis, S.E., Russell, J.M., Heuroux, A.M., D'Andrea, W.J., and Sinninghe Damsté, J.S., 2014, Seasonal variability of branched glycerol dialkyl glycerol tetraethers (brGDGTs) in a temperate lake system: Geochimica et Cosmochimica Acta, v. 144, p. 173–187, <https://doi.org/10.1016/j.gca.2014.08.027>.
- Lu, H., Liu, W., Wang, H., and Wang, Z., 2016, Variation in 6-methyl branched glycerol dialkyl glycerol tetraethers in Lantian loess-paleosol sequence and effect on paleotemperature reconstruction: Organic Geochemistry, v. 100, p. 10–17, <https://doi.org/10.1016/j.orggeochem.2016.07.006>.
- Martin, K.C., Buizert, C., Edwards, J.S., Kalk, M.L., Riddell-Young, B., Brook, E.J., Beaudette, R., Severinghaus, J.P., and Sowers, T.A., 2023, Bipolar impact and phasing of Heinrich-type climate variability: Nature, v. 617, p. 100–104, <https://doi.org/10.1038/s41586-023-05875-2>.
- McManus, J.F., Francois, R., Gherardi, J.-M., Keigwin, L.D., and Brown-Leger, S., 2004, Collapse and rapid resumption of Atlantic meridional circulation

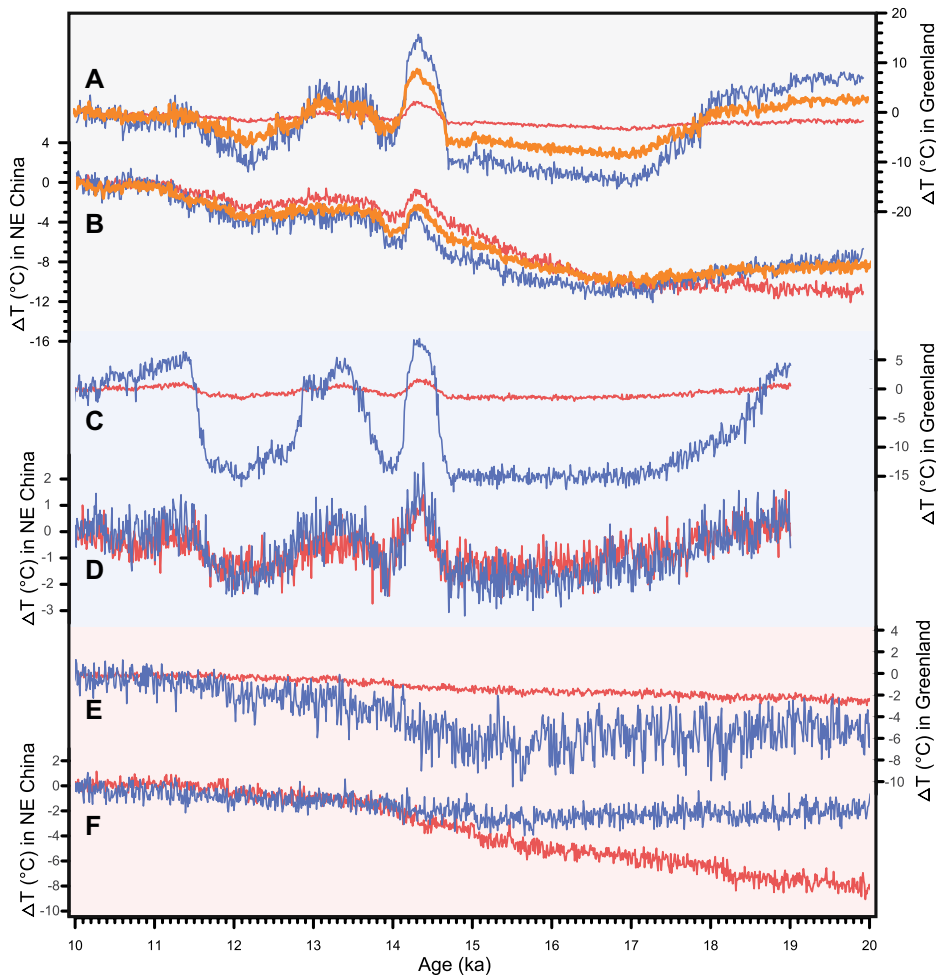


**Figure 4.** TraCE-21ka model simulated summer (June–July–August [JJA], red lines), winter (December–January–February [DJF], blue lines), and mean annual temperature (MAT) changes (orange lines) in Greenland (61.2°N, 45.0°W) and NE China (46.4°N, 120.0°E) based on all forcing factors (A, B), meltwater single forcing (C, D), and orbital single forcing (E, F).

linked to deglacial climate changes: *Nature*, v. 428, p. 834–837, <https://doi.org/10.1038/nature02494>.

Meyer, V.D., Max, L., Hefter, J., Tiedemann, R., and Mollenhauer, G., 2016, Glacial-to-Holocene evolution of sea surface temperature and surface circulation in the subarctic northwest Pacific and the western Bering Sea: *Paleoceanography*, v. 31, p. 916–927, <https://doi.org/10.1002/2015PA002877>.

Mingram, J., et al., 2018, Millennial-scale East Asian monsoon variability of the last glacial deduced from annually laminated sediments from Lake Sihailongwan, N.E. China: *Quaternary Science Reviews*, v. 201, p. 57–76, <https://doi.org/10.1016/j.quascirev.2018.09.023>.

Qian, S., Yang, H., Dong, C., Wang, Y., Wu, J., Pei, H., Dang, X., Lu, J., Zhao, S., and Xie, S., 2019, Rapid response of fossil tetraether lipids in lake sediments to seasonal environmental variables in a shallow lake in central China: Implications for the use of tetraether-based proxies: *Organic Geochemistry*, v. 128, p. 108–121, <https://doi.org/10.1016/j.orggeochem.2018.12.007>.

Repschläger, J., et al., 2021, Active North Atlantic deepwater formation during Heinrich Stadial 1: *Quaternary Science Reviews*, v. 270, <https://doi.org/10.1016/j.quascirev.2021.107145>.

Shakun, J.D., and Carlson, A.E., 2010, A global perspective on Last Glacial Maximum to Holocene climate change: *Quaternary Science Reviews*, v. 29, p. 1801–1816, <https://doi.org/10.1016/j.quascirev.2010.03.016>.

Stebich, M., Rehfeld, K., Schlütz, F., Tarasov, P.E., Liu, J., and Mingram, J., 2015, Holocene vegetation and climate dynamics of NE China based on the pollen record from Sihailongwan maar lake: *Quaternary Science Reviews*, v. 124, p. 275–289, <https://doi.org/10.1016/j.quascirev.2015.07.021>; erratum available at <https://doi.org/10.1016/j.quascirev.2015.09.005>.

Stocker, T.F., 1998, The seesaw effect: *Science*, v. 282, p. 61–62, <https://doi.org/10.1126/science.282.5386.61>.

Sun, Q., Chu, G., Liu, M., Xie, M., Li, S., Ling, Y., Wang, X., Shi, L., Jia, G., and Lü, H.,

2011, Distributions and temperature dependence of branched glycerol dialkyl glycerol tetraethers in recent lacustrine sediments from China and Nepal: *Journal of Geophysical Research*, v. 116, G01008, <https://doi.org/10.1029/2010JG001365>.

Sun, Q., Chu, G., Xie, M., Ling, Y., Su, Y., Zhu, Q., Shan, Y., and Liu, J., 2018, Long-chain alkenone-inferred temperatures from the last deglaciation to the early Holocene recorded by annually laminated sediments of the maar lake Sihailongwan, northeastern China: *The Holocene*, v. 28, p. 1173–1180, <https://doi.org/10.1177/0959683618761546>.

Sun, Y., Oppo, D.W., Xiang, R., Liu, W., and Gao, S., 2005, Last deglaciation in the Okinawa Trough: Subtropical northwest Pacific link to Northern Hemisphere and tropical climate: *Paleoceanography*, v. 20, PA4005, <https://doi.org/10.1029/2004PA001061>.

Svensson, A., et al., 2008, A 60,000 year Greenland stratigraphic ice core chronology: *Climate of the Past*, v. 4, p. 47–57, <https://doi.org/10.5194/cp-4-47-2008>.

Tian, L., Wang, M., Zhang, X., Yang, X., Zong, Y., Jia, G., Zheng, Z., and Man, M., 2019, Synchronous change of temperature and moisture over the past 50 ka in subtropical southwest China as indicated by biomarker records in a crater lake: *Quaternary Science Reviews*, v. 212, p. 121–134, <https://doi.org/10.1016/j.quascirev.2019.04.003>.

Wu, J., Liu, Q., Wang, L., Chu, G., and Liu, J., 2016, Vegetation and climate change during the last deglaciation in the Great Khingan Mountain, northeastern China: *PLoS ONE*, v. 11, <https://doi.org/10.1371/journal.pone.0146261>.

Xu, D., et al., 2023, Fast response of vegetation in East Asia to abrupt climatic events during the last deglaciation: *PNAS Nexus*, v. 2, no. 3, <https://doi.org/10.1093/pnasnexus/pgad061>.

Zhang, S., Xiao, J., and Xu, Q., 2022, Regional precipitation variations during Heinrich events and Dansgaard-Oeschger cycles in the northern margin of the East Asian summer monsoon region: *Quaternary Science Reviews*, v. 278, <https://doi.org/10.1016/j.quascirev.2022.107380>.

Zheng, Y., Pancost, R.D., Liu, X., Wang, Z., Naafs, B.D.A., Xie, X., Liu, Z., Yu, X., and Yang, H., 2017, Atmospheric connections with the North Atlantic enhanced the deglacial warming in northeast China: *Geology*, v. 45, p. 1031–1034, <https://doi.org/10.1130/G39401.1>.

Zhu, Z., Wu, J., Rioual, P., Mingram, J., Yang, H., Zhang, B., Chu, G., and Liu, J., 2021, Evaluation of the sources and seasonal production of brGDGTs in lake Sihailongwan (N.E. China) and application to reconstruct paleo-temperatures over the period 60–8 k.y. B.P.: *Quaternary Science Reviews*, v. 261, <https://doi.org/10.1016/j.quascirev.2021.106946>.

Zhu, Z., Wu, J., Lu, J., Chu, G., Rioual, P., Wang, L., and Liu, J., 2023, Holocene summer temperature record based on branched tetraethers in Northeast China: *The Holocene*, v. 33, p. 1465–1473, <https://doi.org/10.1177/09596836231197769>.

Printed in the USA